Journal of Nuclear Materials 478 (2016) 158–163

Contents lists available at ScienceDirect

Journal of Nuclear Materials

journal homepage: www.elsevier.com/locate/jnucmat

Thermodynamic studies of studtite thermal decomposition pathways via amorphous intermediates UO_3, U_2O_7, and UO_4

Xiaofeng Guo [a], Di Wu [b, c], Hongwu Xu [a], Peter C. Burns [d, e], Alexandra Navrotsky [b, *]

[a] Earth and Environmental Sciences Division, Los Alamos National Laboratory, Los Alamos, NM 87545, United States
[b] Peter A. Rock Thermochemistry Laboratory and NEAT ORU, University of California, Davis, CA 95616, United States
[c] The Gene and Lina Voiland School of Chemical Engineering and Bioengineering, Washington State University, Pullman, WA 99163, United States
[d] Department of Civil and Environmental Engineering and Earth Sciences, University of Notre Dame, Notre Dame, IN 46556, United States
[e] Department of Chemistry and Biochemistry, University of Notre Dame, Notre Dame, IN 46556, United States

ARTICLE INFO

Article history:
Received 21 April 2016
Received in revised form
4 June 2016
Accepted 6 June 2016
Available online 8 June 2016

Keywords:
UO_2
Studtite
Calorimetry
Enthalpy of formation
Nuclear fuel alteration

ABSTRACT

The thermal decomposition of studtite $(UO_2)O_2(H_2O)_2 \cdot 2H_2O$ results in a series of intermediate X-ray amorphous materials with general composition UO_{3+x} ($x = 0, 0.5, 1$). As an extension of a structural study on U_2O_7, this work provides detailed calorimetric data on these amorphous oxygen-rich materials since their energetics and thermal stability are unknown. These were characterized *in situ* by thermogravimetry, and mass spectrometry. *Ex situ* X-ray diffraction and infrared spectroscopy characterized their chemical bonding and local structures. This detailed characterization formed the basis for obtaining formation enthalpies by high temperature oxide melt solution calorimetry. The thermodynamic data demonstrate the metastability of the amorphous UO_{3+x} materials, and explain their irreversible and spontaneous reactions to generate oxygen and form metaschoepite. Thus, formation of studtite in the nuclear fuel cycle, followed by heat treatment, can produce metastable amorphous UO_{3+x} materials that pose the risk of significant O_2 gas. Quantitative knowledge of the energy landscape of amorphous UO_{3+x} was provided for stability analysis and assessment of conditions for decomposition.

© 2016 Elsevier B.V. All rights reserved.

1. Introduction

Studtite, $(UO_2)O_2(H_2O)_2 \cdot 2H_2O$, and metastudtite, $(UO_2)O_2(H_2O)_2$, form as alteration products on spent nuclear fuel (SNF) in aqueous environments [1–3]. They are important where spent fuel is altered during surface or geological storage, in nuclear accidents, and in the processing of uranium ores [1–12]. The formation of studtite in a nuclear waste repository is favorable where H_2O_2 is present under locally oxidative conditions [1,2,4,5], with the H_2O_2 generated and replenished by water radiolysis caused by high radiation dosage [13]. However, as shown by thermodynamic investigations by Kubatko et al. [4] and Guo et al. [11], both studtite and metastudtite have positive enthalpies of formation, 22.3 ± 3.9 and 15.8 ± 1.7 kJ/mol, from γ-UO_3, H_2O and O_2, respectively. This suggests that once studtite or metastudtite form, eventual decomposition may release soluble U(VI) [4,11]. Hence, understanding the decomposition pathway of studtite may help to clarify aspects of UO_2 fuel degradation involving exposure to water. Studtite is often precipitated during production of uranium yellowcake from uranium ore processing, and decomposition of studtite or other uranium peroxides may release O_2 gas during transport and storage [14,15].

The decomposition of studtite upon heating under oxygen or argon atmospheres occurs in several steps [11,15–21]. Irreversible dehydration to metastudtite begins around 60 °C. Continued heating through 200 °C produces an X-ray amorphous material [11,18,21]. The amorphous phase can persist to 550–600 °C under heating rates of 10 °C per minute, beyond which α-$UO_{2.9}$ crystallizes, followed by U_3O_8 at higher temperature [11,17,18]. Among these intermediate decomposition products, the amorphous materials are interesting both because they appear to contain peroxide, and because their structures and reactivity with water are not fully understood [15,21]. Odoh et al. observed the reaction of amorphous uranyl-bearing material, obtained by heating studtite with water [15]: such a reaction may contribute to pressurization of drums containing yellowcake due to the generation of oxygen from the reaction [14,15].

* Corresponding author.
E-mail address: anavrotsky@ucdavis.edu (A. Navrotsky).

http://dx.doi.org/10.1016/j.jnucmat.2016.06.014
0022-3115/© 2016 Elsevier B.V. All rights reserved.

The amorphous nature of materials arising from the heating of studtite is challenging to characterization for structure, composition, and energetics. It has been proposed that amorphous material formed by heating studtite at 195 °C has composition U_2O_7 and contains uranyl and peroxide [15,16]. Other studies assumed this material is $UO_3 \cdot xH_2O$ [11,19,20], although the presence of water was not confirmed. In the most recent study, neutron scattering, spectroscopic measurements, and high-level computational studies demonstrated that heating studtite to 200 °C for 1 h results in a material close in composition to U_2O_7 that may consist of dimeric units of uranyl ions bridged through peroxide and oxo groups [15]. This study also found that the amorphous material continued to lose mass upon heating to higher temperatures, indicating a range of compositions.

In the present work, differential scanning calorimetry (DSC) and thermogravimetric analysis (TGA) coupled with mass spectrometry (MS) have been used to study the thermal decomposition of studtite in detail. Correlating TGA and MS provides further compositional information for amorphous uranyl materials formed during heating. Attenuated total reflectance Fourier transform infrared spectroscopy (ATR-FTIR) was used to characterize uranyl and water in the materials. High temperature oxide melt solution calorimetry was employed to determine formation enthalpies of several amorphous materials with different well-characterized compositions. We also determined these enthalpies of reaction of the amorphous material with water on the basis of new and existing thermochemical data. Our results demonstrate that the reaction of amorphous uranyl materials with water that releases oxygen is exothermic in enthalpy, favorable in free energy, and spontaneous, confirming that these amorphous materials are unstable when exposed to water.

2. Experimental methods

2.1. Materials

All reagents, unless otherwise mentioned, were analytical grade and obtained from Merck KGaA Darmstadt. Studtite was synthesized from an acidic (HCl, pH ~ 3) aqueous UO_2 suspension by slowly adding (one drop per minute) a 30% (wt/wt) H_2O_2 solution to the mixture. After the desired amount had been added, the mixture was stirred for an additional 24 h at room temperature. The obtained light yellow precipitate was filtered, washed with deionized water, and dried at ambient temperature. Finally, metastudtite was obtained by dehydrating the prepared studtite at 90 °C for 48 h.

2.2. Thermal analysis

Differential thermal analysis and differential scanning calorimetry (TG-DSC) were performed simultaneously by heating the sample in a flowing argon atmosphere (40 mL/min) to 800 °C with a rate of 10 °C/min in a Netzsch 449 simultaneous thermal analyzer instrument. A mass spectrometer (Cirrus2) was connected to detect the released gases. The system was calibrated by decomposing CaC_2O_4. Acquired data were processed with the Calisto software package from AKTS. Detailed procedures have been described previously [11,22].

2.3. Infrared spectroscopy

The ATR-FTIR spectra of samples treated at 200 and 400 °C in argon, and their hydrated forms, were recorded in air from 700 to 4000 cm^{-1} employing a Bruker Vertex 70 FTIR spectrometer equipped with an ATR cell with diamond crystal.

2.4. High temperature oxide melt solution calorimetry

High temperature oxide melt solution calorimetry was conducted using a custom built Tian-Calvet twin microcalorimeter [23,24]. Powdered samples were hand pressed into small pellets (~5 mg) before heating in a furnace to the desired temperature. Subsequently, the pellets were quickly cooled and were dropped from room temperature into molten solvent (20 g of sodium molybdate ($3Na_2O \cdot 4MoO_3$)) in a Pt crucible at 702 °C. The calorimeter was calibrated using the heat content of ~5 mg α-Al_2O_3 pellets [23,24]. Oxygen gas was continuously bubbled through the melt at 5 mL/min to ensure an oxidizing environment and facilitate dissolution [25]. Flushing oxygen gas at ~50 mL/min through the calorimeter chamber assisted in maintaining a constant gas environment above the solvent [25]. Dissolution of uranium oxides and other uranium-containing compounds as U^{6+} species has been demonstrated in this solvent, and their drop solution enthalpy data were obtained previously [10,11,22,26–28]. Upon rapid and complete dissolution of the sample, the enthalpy of drop solution, ΔH_{ds}, was obtained. Finally, using appropriate thermochemical cycles (Table 2), enthalpies of formation of the amorphous materials from constituent oxides, $\Delta H_{f,ox}$ were calculated.

3. Results and discussion

Stepwise decomposition of studtite was observed during heating in the thermal analyzer: $(UO_2)O_2(H_2O)_2 \cdot 2H_2O \rightarrow (UO_2)O_2(H_2O)_2 \rightarrow$ amorphous uranyl phases → amorphous -UO_3 → α-$UO_{2.9}$ → U_3O_8 (Fig. 1). The mass loses are associated with release of oxygen and/or water, as shown by the MS peaks. Quenched samples from 210, 300, 400, 535, and 580 °C are labeled as sample A, B-1, B-2, C, and D, respectively. The resulting materials have different colors (Fig. 2). X-ray diffraction demonstrated that A is an incomplete decomposition product of metastudtite (Fig. 3). B-1 and B-2 were quenched after heating into the region of the TG that corresponds to a wide plateau (Fig. 1). Sample C was retrieved after heating to 535 °C and was identified as *am*-UO_3 by comparing TG data with calculated theoretical mass loss [11]. C is bright orange and is free of water (Fig. 2, Table 1), consistent with the previous study [11]. Samples B-1, B-2, and C are X-ray amorphous. Sample D is crystalline α-$UO_{2.9}$ [11]. Further heating leads to partial reduction of the uranium and transformation of α-$UO_{2.9}$ to U_3O_8 [11,19,20].

TGA and *in situ* MS revealed only two water peaks, associated with the decomposition of studtite and of metastudtite, both of which contain H_2O (Fig. 1), consistent with the amorphous uranyl compounds being anhydrous. Around 200 °C, the MS shows an oxygen peak accompanying decomposition of metastudtite, indicating that the initial X-ray amorphous decomposition product has less oxygen than metastudtite. The next oxygen signal in the MS was observed upon heating above 500 °C, where *am*-UO_3 (sample C) formed. Thus, samples B-1, B-2, and other amorphous uranyl materials formed below 500 °C are less oxygen-rich than metastudtite but more oxygen-rich than UO_3. Two small MS oxygen peaks occur from 535 to 580 °C and 610–660 °C, corresponding to the conversions *am*-UO_3 → α-$UO_{2.9}$, and α-$UO_{2.9}$ → U_3O_8, respectively.

The IR spectrum of B-2 in Fig. 4 contains strong broad peaks centered around 901 and 740 cm^{-1}, attributable to the stretching vibrations of uranyl in the amorphous uranium oxides, as reported by Sato et al. [21]. No peaks related to OH or H_2O stretching or bending modes were observed, confirming this amorphous material is free of structural water. The mass losses for forming B-1 and B-2 from studtite are 18.39 and 19.91%, respectively, indicating that these two samples have different compositions. Combining the results from TGA and IR analysis and considering charge neutrality,

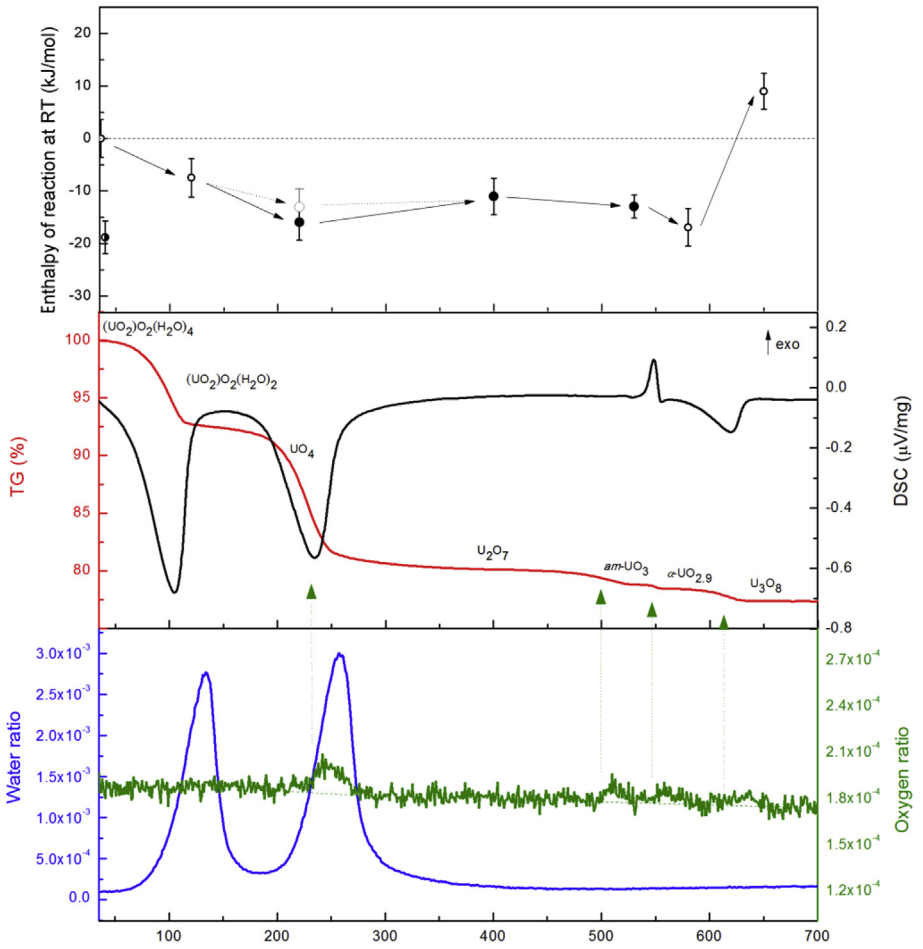

Fig. 1. Decomposition of studtite in Ar at elevated temperatures: TG trace is the red curve; DSC trace is the black curve; Water MS signal is the blue curve; Oxygen MS signal is the green curve. The top figure shows the enthalpy of reaction of studtite to each of intermediate/final products retrieved at different temperatures: filled circles are from this work, open black circles are from Refs. [4,11,30], the open grey circle is estimated to be UO_4 (see discussion), and the half-filled circle represents the reaction enthalpy from studtite to metaschoepite [31]. (For interpretation of the references to color in this figure legend, the reader is referred to the web version of this article.)

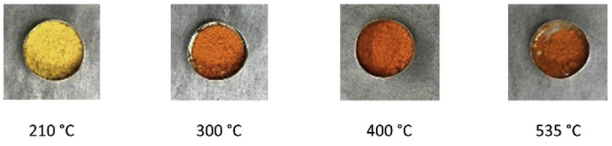

Fig. 2. Samples retrieved from indicated temperatures display different colors. (The sample from 210 °C if was heated continuously at 200 °C for 4 h turned a color similar to that of the sample at 300 °C).

we conclude that the stoichiometric formula of samples B may have one uranyl group, one peroxide group, and one-half an oxo group: $(UO_2)OO_{0.5}$, or, otherwise stated, as *am*-U_2O_7, consistent with the findings of Odoh et al. [15] and Boggs et al. [16].

The transition from $(UO_2)O_2(H_2O)_2$ to *am*-U_2O_7 involves dehydration and loss of oxygen; however, only one DSC peak is observed. The heat effect of losing oxygen may be small and overshadowed by the dominating endothermic dehydration peak, with the loss of water and oxygen occurring simultaneously, as loss of one or the other would destabilize the structure of metastudtite. Alternatively, during the decomposition of metastudtite, release of water could occur before oxygen loss, giving a narrow temperature range of *am*-UO_4. Studtite was heated at 200 °C for 4 h in an attempt to dehydrate the material while preserving all peroxide (MS trace, Fig. 1). The retrieved material was denoted sample E. Unlike sample A that was quenched from 210 °C after being heated to that temperature for a short time and for which the X-ray diffraction pattern indicated remaining crystallinity, sample E is X-ray amorphous (Fig. S1). During the heating process, the integral of the water MS peak of the second dehydration is similar to that from a prior DSC-TG experiment that directly heated the sample to 800 °C (MS integral values: 0.27 vs. 0.28 arbitrary units). This indicates that water was mostly or entirely removed during heating to form sample E. In addition, the mass change from studtite to sample E is 17.9%, smaller than that from studtite to sample B-2. This mass loss is mostly attributable to excess oxygen, but may also be partly due to some residual OH or H_2O. As shown in the IR spectrum (Fig. 4), a detectable amount of H_2O remains in sample E; a small broad peak at 3520–3150 cm^{-1} and a small sharp peak at 1607 cm^{-1} correspond to H_2O stretching and bending bands, respectively. These findings are consistent with the NMR data of Odoh et al. [15]. This small H_2O content is difficult to quantify, but will be reflected in the derived formation enthalpy from calorimetric experiments (see below). The IR spectrum of sample E shows similar uranyl stretching modes as sample B-2. Hence, we conclude that sample E is an amorphous material with uranyl ions and is similar to samples B, but somewhat more oxygen-rich and containing a small amount of H_2O. It is an intermediate material that occurs in the pathway from metastudtite, $(UO_2)O_2(H_2O)_2$ to *am*-U_2O_7. Considering the residual H_2O and the TG result, sample E has a chemical formula

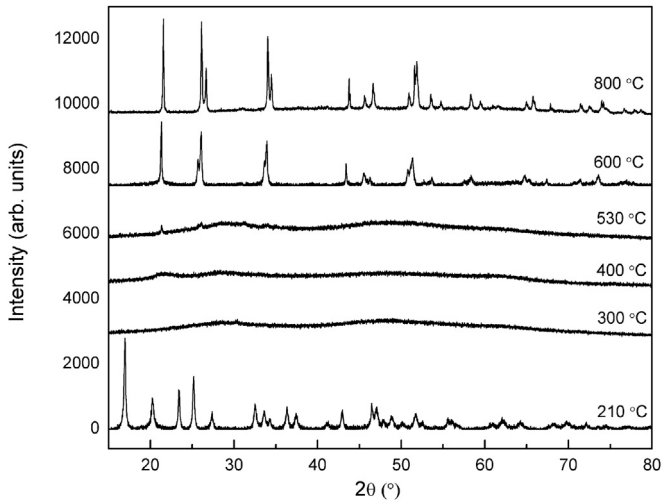

Fig. 3. Powder X-ray diffraction patterns of samples retrieved from different temperatures. The samples quenched from 210 °C still have metastudtite. Continuing heating at 200 °C for 4 h causes complete amorphization (Fig. S2). The sample heated to 580 °C is α-$UO_{2.9}$ (PDF 18–1427); and 800 °C is U_3O_8 (PDF 61–2801). Patterns at 300, 530, and 800 °C are from the literature [11].

that can be approximated by $(UO_2)O_{(2-x)}(H_2O)_y$, and this formula was used in our thermochemical analysis.

Measured drop solution enthalpies, ΔH_{ds}, are used in thermochemical cycles (Table 2) to derive $\Delta H_{f,ox}$. The reaction to form sample E from its binary oxides is approximated as

$$\gamma\text{-}UO_{3(s,\ 25\ ^\circ C)} + yH_2O_{(l,\ 25\ ^\circ C)} + (1-x)/2O_{2(g,\ 25\ ^\circ C)} \rightarrow (UO_2)O_{(2-x)}(H_2O)_{y(s,\ 25\ ^\circ C)} \quad (1)$$

$\Delta H_{f,ox}$ of sample E was derived based on $x = 0.1$, and $y = 0$ or 0.1, which were estimated from TG. When $y = 0$, sample E was assumed to be free of H_2O and its formula is $(UO_2)(O_{2-x})$. The obtained $\Delta H_{f,ox}$(sample E, $y = 0$) is 6.2 ± 3.0 kJ/mol. If the sample has 10 mol % H_2O ($y = 0.1$), it has a slightly more endothermic enthalpy of formation, 13.1 ± 3.0 kJ/mol. Thus there is a slight positive shift in $\Delta H_{f,ox}$ with increasing H_2O content, but this change is not clearly beyond experimental error. $\Delta H_{f,ox}$ for *am*-U_2O_7 and *am*-UO_3 are 11.6 ± 1.7 and 10.3 ± 1.5 kJ/mol, considering the reactions of forming sample B-2 and C shown below as (2) and (3), respectively,

$$\gamma\text{-}UO_{3(s,\ 25\ ^\circ C)} + 1/4O_{2(g,\ 25\ ^\circ C)} \rightarrow am\text{-}U_2O_{7\ (s,\ 25\ ^\circ C)} \quad (2)$$

$$\gamma\text{-}UO_{3(s,\ 25\ ^\circ C)} \rightarrow am\text{-}UO_{3\ (s,\ 25\ ^\circ C)} \quad (3)$$

The small positive formation enthalpy values, corresponding to small negative decomposition enthalpies, confirm the expected metastable nature of these amorphous phases. Since their decomposition evolves oxygen gas, the entropy of the reaction is positive, so, with negative enthalpy and positive entropy, decomposition is thermodynamically favored and spontaneous.

The obtained thermodynamic data establish an energy landscape for studtite decomposition products by considering the reactions from studtite to each phase. The enthalpies of reaction (ΔH_{rxn}) are shown in Table 3 and Fig. 1. Studtite decomposes into gradually more stable phases. ΔH_{rxn} of sample E was estimated based on H_2O free ($y = 0$, black circle in Fig. 1), and residual H_2O

Table 1
TG analysis in O_2 correlating experimental and theoretical weight loss (%).

Step	Experimental weight loss (%)	Theoretical weight loss (%)	Difference δ (%)
1. $(UO_2)O_2(H_2O)_2{\cdot}2H_2O \rightarrow (UO_2)O_2(H_2O)_2$	7.4	9.6	2.2
2. $(UO_2)O_2(H_2O)_2{\cdot}2H_2O \rightarrow (UO_2)O_{(2-x)}(H_2O)_y$ (sample E)	17.9	19.3	2.2[a]
3. $(UO_2)O_2(H_2O)_2{\cdot}2H_2O \rightarrow (UO_2)OO_{0.5}$ (sample B-2)	19.4	21.6	2.2[a]
4. $(UO_2)O_2(H_2O)_2{\cdot}2H_2O \rightarrow$ *am*-UO_3 (Sample C)	21.2	23.5	2.3
5. $(UO_2)O_2(H_2O)_2{\cdot}2H_2O \rightarrow$ α-$UO_{2.9}$ (Sample D)	21.7	24.0	2.2
6. $(UO_2)O_2(H_2O)_2{\cdot}2H_2O \rightarrow U_3O_8$	22.7	25.0	2.3

[a] Averaging over δ from the other steps (1, 4, 5, and 6).

Table 2
Thermochemical cycles of *am*-UO_{3+x} ($x = 0$, 0.5, 1).

Reaction	ΔH (kJ/mol)
Enthalpies of formation of ***am-UO$_{3+x}$*** *from the binary oxides ($\Delta H_{f,ox}$) at 25 °C*	
(1) (Sample E) $(UO_2)O_{(2-x)}(H_2O)_{y\ (s,\ 25\ ^\circ C)} \rightarrow UO_{3(sln,\ 702\ ^\circ C)} + yH_2O_{(g,\ 702\ ^\circ C)} + (1-x)/2O_{2(g,\ 702\ ^\circ C)}$	$\Delta H_1 = \Delta H_{ds} = 13.11$[a] ± 2.55[b](4)[c]
(2) (Sample B-2) $(UO_2)OO_{0.5(s,\ 25\ ^\circ C)} \rightarrow UO_{3(sln,\ 702\ ^\circ C)} + 0.5/2O_{2(g,\ 702\ ^\circ C)}$	$\Delta H_2 = \Delta H_{ds} = 2.77 \pm 0.76(4)$
(3) *am*-$UO_{3(s,\ 25\ ^\circ C)} \rightarrow UO_{3(sln,\ 702\ ^\circ C)}$	$\Delta H_3 = \Delta H_{ds} = -0.77 \pm 0.06(3)$
(4) γ-$UO_{3(sln,\ 702\ ^\circ C)} \rightarrow UO_{3(sln,\ 702\ ^\circ C)}$	$\Delta H_4 = 9.49 \pm 1.53(13)$ [22,26]
(5) $O_{2(g,\ 25\ ^\circ C)} \rightarrow O_{2(g,\ 702\ ^\circ C)}$	$\Delta H_5 = 21.83$ [29]
(6) $H_2O_{(l,\ 25\ ^\circ C)} \rightarrow H_2O_{(g,\ 702\ ^\circ C)}$	$\Delta H_6 = 69.0$ [29]
(7) $\gamma\text{-}UO_{3(s,\ 25\ ^\circ C)} + (1-y)/2H_2O_{(l,\ 25\ ^\circ C)} + (1+y)/4O_{2(g,\ 25\ ^\circ C)} \rightarrow (UO_2)O_{(1+y)}(OH)_{(1-y)(s,\ 25\ ^\circ C)}$	$\Delta H_7 = \Delta H_{f,ox}$
(8) $\gamma\text{-}UO_{3(s,\ 25\ ^\circ C)} + 1/4O_{2(g,\ 25\ ^\circ C)} \rightarrow (UO_2)OO_{0.5(s,\ 25\ ^\circ C)}$	$\Delta H_8 = \Delta H_{f,ox}$
(9) $\gamma\text{-}UO_{3(s,\ 25\ ^\circ C)} \rightarrow$ *am*-$UO_{3\ (s,\ 25\ ^\circ C)}$	$\Delta H_9 = \Delta H_{f,ox}$
Enthalpy of formation of UO_{3+x} from γ-UO_3 and O_2	
$\Delta H_{f,ox}((UO_2)O_{(2-x)}(H_2O)_y) = -\Delta H_1 + \Delta H_4 + (1-x)/4\ \Delta H_5 + y\ \Delta H_6$	
$= 6.2 \pm 3.0$ kJ/mol ($y = 0$)	
$= 13.1 \pm 3.0$ kJ/mol ($y = 0.1$)	
$\Delta H_{f,ox}((UO_2)OO_{0.5}) = -\Delta H_2 + \Delta H_4 + 0.5/2\ \Delta H_5$	
$= 11.6 \pm 1.7$ kJ/mol	
$\Delta H_{f,ox}$(*am*-UO_3) $= -\Delta H_3 + \Delta H_4 = 10.3 \pm 1.5$ kJ/mol	

[a] Average.
[b] Two standard deviations of the average value.
[c] Number of measurements.

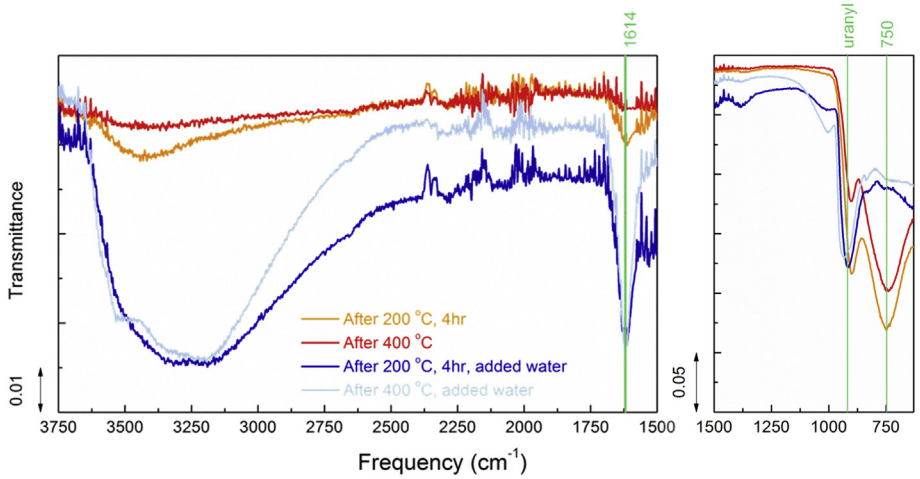

Fig. 4. IR spectra of sample B-2 (after 400 °C heating), and its product after reacting with water; of sample E (after 200 °C heating for 4 h), and its product after reaction with water.

Table 3
Enthalpies of reaction from studtite to decomposing products at 25 °C.

Step[a]	ΔH_{rxn} (kJ/mol)
1. $(UO_2)O_2(H_2O)_2{\cdot}2H_2O \rightarrow (UO_2)O_2(H_2O)_2 + 2H_2O$	−7.4 ± 3.7
2. $(UO_2)O_2(H_2O)_2{\cdot}2H_2O \rightarrow (UO_2)O_{(2-x)}(H_2O)_y + (4-y)\ H_2O + x/2\ O_2$	−17.0 ± 3.4
3. $(UO_2)O_2(H_2O)_2{\cdot}2H_2O \rightarrow (UO_2)OO_{0.5} + 4\ H_2O + 1/4\ O_2$	−11.6 ± 3.4
4. $(UO_2)O_2(H_2O)_2{\cdot}2H_2O \rightarrow am\text{-}UO_3 + 4\ H_2O + 1/2\ O_2$	−13.0 ± 2.3
5. $(UO_2)O_2(H_2O)_2{\cdot}2H_2O \rightarrow \alpha\text{-}UO_{2.9} + 4\ H_2O + 1.1/2\ O_2$	−16.9 ± 3.6
6. $(UO_2)O_2(H_2O)_2{\cdot}2H_2O \rightarrow 1/3\ U_3O_8 + 4\ H_2O + 2/3\ O_2$	9.0 ± 3.4

[a] These values are plotted in Fig. 1.

($y = 0.1$, grey open circle in Fig. 1). This H_2O content correction is relatively small. Similar reaction energetics relative to studtite are found for the amorphous UO_x phases: −10.1 ± 3.4 kJ/mol for UO_4, −11.6 ± 3.4 kJ/mol for *am*-U_2O_7, and −13.0 ± 2.3 kJ/mol for *am*-UO_3. The relatively small energetic differences among these amorphous phases are consistent with the observations from DSC (Fig. 1), which show no peaks between 250 and 500 °C. These metastable amorphous phases crystallize into α-$UO_{2.9}$. The DSC trace around 530 °C shows an exothermic heat effect, confirming the lower energy of the crystalline uranyl phase compared to the amorphous uranyl material, consistent with results from high temperature solution calorimetry. The final decomposition involving oxygen loss and reduction of some of the U to give U_3O_8 is reflected by the large endothermic effect shown by DSC.

Although the anhydrous amorphous uranyl materials that result from heating studtite are more stable than either studtite or metastudtite, *am*-U_2O_7 is known to react with water and generate oxygen [15]. Adding water to samples E, B, and C causes all to react and form metaschoepite ($UO_3{\cdot}2H_2O$), a common hydrated uranyl mineral. Samples with approximate compositions UO_4 and am-U_2O_7 interact with water quite rapidly. Bubbles occur immediately after contact with water [15]. A much slower recrystallization process occurs for *am*-UO_3 in water, which is consistent with its lack of peroxide: the sample remained amorphous even 2 h after water was added, but it had formed metaschoepite (Fig. S2) after 12 h. The general reaction of the amorphous UO_{3+x} materials with water can be expressed as:

$$am\text{-}UO_{3+x} + nH_2O \rightarrow UO_3{\cdot}nH_2O + x/2\ O_2 \quad (4)$$

The derived enthalpies of reaction from B, E, and *am*-UO_3, to $UO_3{\cdot}2H_2O$ at 25 °C are −8.7 ± 4.5, −7.2 ± 3.8, and −5.9 ± 3.8 kJ/mol, respectively (Table S2). Thus these reactions are modestly exothermic in enthalpy. They should have strongly positive entropies because gas is produced (except in the case of *am*-UO_3), so their free energies will be more exothermic than their enthalpies. Thus the formation of metaschoepite upon contact with water with the concomitant release of oxygen is thermodynamically favored and spontaneous for the peroxide-bearing amorphous uranyl materials, as observed experimentally.

The IR spectra of samples after reaction with water reveal the presence of water. In both spectra there is a broad stretching band (3535–3150 cm^{-1}) indicating H bonding, and a sharp H_2O bending mode (1614 cm^{-1}). The asymmetric vibrations indicative of the uranyl group (Fig. 4) now are located only at 933 - 914 cm^{-1}, indicating that the uranyl bonding environment for samples B and E are different from that for metaschoepite, as also concluded earlier [15].

The spontaneity of reaction (4) has important implications. Once an amorphous uranyl peroxide forms, its reaction with water leads to the release of oxygen and formation of relatively soluble uranyl phases. During *in situ* mining of uranium, studtite is typically precipitated to recover uranium from an acidic aqueous solution. Subsequently, the studtite is heated to remove water, giving the yellowcake that is destined for shipment and eventual processing. We earlier noted the presence of X-ray amorphous uranyl materials in yellowcake from a drum that had pressurized [15]. The current study confirms that inadvertent or intentional production of amorphous uranyl peroxides by heat treatment of studtite or metastudtite presents a potential hazard because of the possibility of eventual spontaneous release of O_2 gas.

Acknowledgements

Calorimetric studies at UC Davis and data analysis were supported by the Materials Science of Actinides, an Energy Frontier

Research Center funded by the U.S. Department of Energy, Office of Science, Office of Basic Energy Sciences under Award DESC0001089. X. G was supported by a Seaborg postdoctoral fellowship from the Laboratory Directed Research and Development (LDRD) program, through the G. T. Seaborg Institute, of Los Alamos National Laboratory (LANL), which is operated by Los Alamos National Security LLC, under DOE Contract DE-AC52-06NA25396. We thank Sabrina Labs and Dirk Bosbach for providing the initial studtite sample.

Appendix A. Supplementary data

Supplementary data related to this article can be found at http://dx.doi.org/10.1016/j.jnucmat.2016.06.014.

References

[1] G. Sattonnay, C. Ardois, C. Corbel, J.F. Lucchini, M.F. Barthe, F. Garrido, D. Gosset, Alpha-radiolysis effects on UO_2 alteration in water, J. Nucl. Mater 288 (1) (2001) 11–19.
[2] M. Amme, Contrary effects of the water radiolysis product H2O2 upon the dissolution of nuclear fuel in natural ground water and deionized water, Radiochim. Acta 90 (7) (2002) 399–406.
[3] B. Hanson, B. McNamara, E. Buck, J. Friese, E. Jenson, K. Krupka, B. Arey, Corrosion of commercial spent nuclear fuel. 1. Formation of studtite and metastudtite, Radiochim. Acta 93 (3) (2005) 159–168.
[4] K.-A.H. Kubatko, K.B. Helean, A. Navrotsky, P.C. Burns, Stability of peroxide-containing uranyl minerals, Science 302 (5648) (2003) 1191–1193.
[5] B. McNamara, E. Buck, B. Hanson, Observation of studtite and metastudtite on spent fuel, Mater. Res. Soc. Symp. P 757 (2003) 401–406.
[6] F. Clarens, J. De Pablo, I. Diez-Perez, I. Casas, J. Gimenez, M. Rovira, Formation of studtite during the oxidative dissolution of UO_2 by hydrogen peroxide: a SFM study, Environ. Sci. Technol. 38 (24) (2004) 6656–6661.
[7] T.Z. Forbes, P. Horan, T. Devine, D. McInnis, P.C. Burns, Alteration of dehydrated schoepite and soddyite to studtite, $[(UO_2)(O^-{}_2)(H_2O)(_2)](H_2O)(_2)$, Am. Mineral. 96 (1) (2011) 202–206.
[8] P.C. Burns, R.C. Ewing, A. Navrotsky, Nuclear fuel in a reactor accident, Science 335 (6073) (2012) 1184–1188.
[9] C.R. Armstrong, M. Nyman, T. Shvareva, G.E. Sigmon, P.C. Burns, A. Navrotsky, Uranyl peroxide enhanced nuclear fuel corrosion in seawater, Proc. Natl. Acad. Sci. U. S. A. 109 (6) (2012) 1874–1877.
[10] A. Navrotsky, T. Shvareva, X. Guo, Thermodynamics of uranium minerals and related materials, in: P.C. Burns, G.E. Sigmon (Eds.), Uranium - Cradle to Grave, Mineralogical Association of Canada, 2013, pp. 147–164.
[11] X. Guo, S.V. Ushakov, S. Labs, H. Curtius, D. Bosbach, A. Navrotsky, Energetics of metastudtite and implications for nuclear waste alteration, Proc. Natl. Acad. Sci. 111 (50) (2014) 17737–17742.
[12] P.F. Weck, E. Kim, E.C. Buck, On the mechanical stability of uranyl peroxide hydrates: implications for nuclear fuel degradation, RSC Adv. 5 (96) (2015) 79090–79097.
[13] D. Bodansky, Nuclear Energy: Principles, Practices, and Prospects, American Institute of Physics, Woodbury, N.Y, 1996.
[14] Exothermic reactions involving dried uranium oxide powder (yellowcake), U.S. Nuclear Regulatory Commission, 2014.
[15] S.O. Odoh, J. Shamblin, C.A. Colla, S. Hickam, H.L. Lobeck, R.A.K. Lopez, T. Olds, J.E.S. Szymanowski, G.E. Sigmon, J. Neuefeind, W.H. Casey, M. Lang, L. Gagliardi, P.C. Burns, Structure and reactivity of X-ray amorphous uranyl peroxide, U_2O_7, Inorg. Chem. 55 (7) (2016) 3541–3546.
[16] J.E. Boggs, M. El-Chehabi, The thermal decomposition of uranium peroxide, $UO_4 \cdot 2H_2O$, J. Am. Chem. Soc. 79 (16) (1957) 4258–4260.
[17] E.H.P. Cordfunke, Alpha-UO_3 - its preparation and thermal stability, J. Inorg. Nucl. Chem. 23 (3–4) (1961) 285–286.
[18] E.H.P. Cordfunke, A.A. Vandergiessen, Pseudomorphic decomposition of uranium peroxide into UO_3, J. Inorg. Nucl. Chem. 25 (5) (1963) 553–558.
[19] E.H.P. Cordfunke, P. Aling, Thermal decomposition of hydrated uranium peroxides, Recl, Trav. Chim. Pay. B 82 (3) (1963) 257–263.
[20] C. Rocchicc, Etude Par Thermogravimetrie analyse thermique differentielle et spectrographie dabsorption infrarouge des hydrates du peroxyde duranium, Cr. Acad. Sci. B Phys. 263 (19) (1966) 1061–1063.
[21] T. Sato, Thermal-decomposition of uranium peroxide hydrates, J. Appl. Chem. Biotechn 26 (4) (1976) 207–213.
[22] X. Guo, S. Szenknect, A. Mesbah, S. Labs, N. Clavier, C. Poinssot, S.V. Ushakov, H. Curtius, D. Bosbach, R.C. Ewing, P.C. Burns, N. Dacheux, A. Navrotsky, Thermodynamics of formation of coffinite, $USiO_4$, Proc. Natl. Acad. Sci. U. S. A. 112 (21) (2015) 6551–6555.
[23] A. Navrotsky, Progress and new directions in high-temperature calorimetry, Phys. Chem. Min. 2 (1–2) (1977) 89–104.
[24] A. Navrotsky, Progress and new directions in high temperature calorimetry revisited, Phys. Chem. Min. 24 (3) (1997) 222–241.
[25] A. Navrotsky, R.P. Rapp, E. Smelik, P. Burnley, S. Circone, L. Chai, K. Bose, The behavior of H_2O and CO_2 in high-temperature lead borate solution calorimetry of volatile-bearing phases, Am. Mineral. 79 (11–12) (1994) 1099–1109.
[26] K.B. Helean, A. Navrotsky, E.R. Vance, M.L. Carter, B. Ebbinghaus, O. Krikorian, J. Lian, L.M. Wang, J.G. Catalano, Enthalpies of formation of Ce-pyrochlore, $Ca_{0.93}Ce_{1.00}Ti_{2.035}O_{7.00}$, U-pyrochlore, $Ca_{1.46}U^{4+}_{0.23}U^{6+}_{0.46}Ti_{1.85}O_{7.00}$ and Gd-pyrochlore, $Gd_2Ti_2O_7$: three materials relevant to the proposed waste form for excess weapons plutonium, J. Nucl. Mater 303 (2–3) (2002) 226–239.
[27] X. Guo, E. Tiferet, L. Qi, J.M. Solomon, A. Lanzirotti, M. Newville, M.H. Engelhard, R.K. Kukkadapu, D. Wu, E.S. Ilton, M. Asta, S. Sutton, H. Xu, A. Navrotsky, U(V) in metal uranates: a combined experimental and theoretical study of $MgUO_4$, $CrUO_4$ and $FeUO_4$, Dalton Trans. 45 (11) (2016) 4622–4632.
[28] X. Guo, A. Navrotsky, R.K. Kukkadapu, M.H. Engelhard, A. Lanzirotti, M. Newville, E.S. Ilton, S. Sutton, H. Xu, Structure and thermodynamics of uranium containing iron garnets, Geochim. Cosmochim. Acta (2016) accepted.
[29] M.W.J. Chase, NIST-JANAF thermochemical tables, fourth edition, J. Phys. Chem. Ref. Data Monogr. 9 (1998) 1–1951.
[30] I. Grenthe, J. Fuger, R.J.M. Konings, R.J. Lemire, A.B. Muller, C. Nguyen-Trung, H. Wanner, Chemical Thermodynamics of Uranium, Elsevier, Amsterdam, 1992.
[31] D. Gorman-Lewis, J.B. Fein, P.C. Burns, J.E.S. Szymanowski, J. Converse, Solubility measurements of the uranyl oxide hydrate phases metaschoepite, compreignacite, Na-compreignacite, becquerelite, and clarkeite, J. Chem. Thermodyn. 40 (2008) 980–990.